

# A Game Between Two Identical Dubins Cars: Evading a Conic Sensor in Minimum Time

Ubaldo Ruiz

**Abstract**—A fundamental task in mobile robotics is keeping an intelligent agent under surveillance with an autonomous robot as it travels in the environment. This work studies a version of that problem involving one of the most popular vehicle platforms in robotics. In particular, we consider two identical Dubins cars moving on a plane without obstacles. One of them plays as the pursuer, and it is equipped with a limited field-of-view detection region modeled as a semi-infinite cone with its apex at the pursuer's position. The pursuer aims to maintain the other Dubins car, which plays as the evader, as much time as possible inside its detection region. On the contrary, the evader wants to escape as soon as possible. In this work, employing differential game theory, we find the time-optimal motion strategies near the game's end. The analysis of those trajectories reveals the existence of at least two singular surfaces: a Transition Surface and an Evader's Universal Surface. We also found that the barrier's standard construction produces a surface that partially lies outside the playing space and fails to define a closed region, implying that an additional procedure is required to determine all configurations where the evader escapes.

**Index Terms**—Pursuit-evasion, Differential Games, Optimal Control.

## I. INTRODUCTION

A fundamental task in mobile robotics is keeping an intelligent agent under surveillance with an autonomous robot as it travels in the environment. This task can be modeled as a pursuit-evasion game with two players having antagonistic goals. In this work, we study a version of a surveillance pursuit-evasion problem considering one of the most commonly used vehicle models in robotics, a Dubins car. In our problem, two identical Dubins cars move on a plane without obstacles. One plays as the pursuer, aiming to keep the other player inside its limited field of view. Having an opposite goal, the evader seeks to escape from it as soon as possible. The pursuer's detection region is modeled as a semi-infinite cone with its apex at the pursuer's position.

We model the problem as a zero-sum differential game. In particular, by performing a retro-time integration starting from the game's terminal conditions, we compute the players' motion strategies near the end of it. The analysis of the corresponding trajectories reveals the existence of at least

two singular surfaces: a Transition Surface and an Evader's Universal Surface. Additionally, by performing the standard barrier's construction to solve the problem of deciding the game's winner, we found that it produces a surface that partially lies outside the playing space and fails to divide it. This suggests that either 1) the evader can escape from all initial positions in the playing space, in which case additional singular surfaces and their corresponding trajectories need to be found to fill the entire space, or 2) the playing space is divided into two regions by other semi-permeable surfaces that emerge from constructing additional singular surfaces. In one, the evader wins, and in another does not.

As was mentioned, we model our problem as a zero-sum differential game. Rufus Isaacs [1] developed a methodology to solve differential games, which is employed in this paper. The fundamental idea is partitioning the playing space into regions where the value function is differentiable. Usually, the process's most challenging part is identifying the regions' boundaries, called *singular surfaces*. Characterizing a singular surface and its outcome is frequently based on the premise that one player must base his control choice on the knowledge of his opponent's control selection. A strategy computed employing this information is called a non-admissible strategy. In contrast, an admissible strategy does not demand further information on the players' controls and is established only on knowledge of the system's state. In our work, we succeed in finding mathematical equations describing the players' time-optimal motion strategies near the game's end and reaching two types of singular surfaces. Refer to [1], [2], [3], for a detailed study of Isaacs' methodology and singular surfaces.

This article is organized as follows. The related work and contributions are presented in Section II, and the problem definition is introduced in Section III. The set of configurations where the game ends is computed in Section IV. In Section V, the players' time-optimal motion strategies near the game's end are obtained. In Section VI, an attempt to solve the decision problem is described, and it is exhibited that it produces a barrier surface that partially lies outside the playing space. A brief discussion about the players' motion strategies and the corresponding trajectories found in this work is presented in Section VII. A numerical simulation illustrating the players' motion strategies is shown in Section VIII, and the conclusions and future work are described in Section IX.

## II. RELATED WORK

This paper studies a pursuit-evasion game [4]. In the literature, many works have addressed pursuit-evasion games

Manuscript received: xxxx, xx, 20xx; Revised xxxx, xx, 20xx; Accepted xxxx, xx, 20xx.

This paper was recommended for publication by Editor xxxx upon evaluation of the Associate Editor and Reviewers' comments. This work was supported by CONACYT grant A1-S-21934.

<sup>2</sup>U. Ruiz is with the Centro de Investigación Científica y de Educación Superior de Ensenada (CICESE), 22860, Baja California, México, uruiz@cicese.mx

Digital Object Identifier (DOI): see top of this page.

[1], [2], [3], [5]. Usually, they are grouped into three main categories: search [6], [7], [8], capture [4], [9], [10], [11], [12], [13], [14], [15], [16], and tracking [17], [18], [19], [20], [21], [22], [23], [24], [25], [26]. In the first category, the pursuer's objective is to find the evader while both players move in an environment with obstacles, i.e., put the evader inside the pursuer's detection region. In the second category, the pursuer strives to capture the evader by attaining a certain distance from it. In this category, usually, the capture wants to be achieved as soon as possible. In the third category, the pursuer's goal is to keep surveillance of the evader as both players advance in the environment, i.e., maintain the evader inside the pursuer's detection region. The problem addressed in this paper belongs to the last category. For a more detailed taxonomy of pursuit-evasion problems, we refer the reader to the following surveys [27], [28]. In the next paragraphs, we summarize and briefly compare the works most related to this paper in differential games' literature. To the best of our knowledge, we believe those works are [26], [29], [30], [31].

In [26], the pursuit-evasion game of surveillance evasion between two identical Differential Drive Robots is studied. In that problem, one of the Differential Drive Robots plays as the pursuer, and it is equipped with a bounded range sensor modeled as a circle centered at the pursuer's location. Similar to our current work, the pursuer's objective is to maintain surveillance of the evader as much as possible while the evader seeks to escape as soon as possible. In that work, the problem of deciding the game's winner, i.e., whether the evader escapes or not, is solved. Additionally, the players' time-optimal strategies when the evader escapes surveillance are provided. Note that our problem differs from [26] in two ways: 1) the players are Dubins cars, which have different time-optimal motion primitives than a Differential Drive Robot, and 2) in our case, the sensor is a semi-infinite cone and not a circle. Those two changes result in the motion strategies and the conditions deciding the game's winner not being the same, requiring a completely new analysis.

In [29], the problem of keeping surveillance of an Omnidirectional Agent with a Differential Drive Robot equipped with a limited field of view sensor is analyzed. Similar to our current work, the sensor is modeled as a semi-infinite cone fixed to the Differential Drive Robot's body. However, since the pursuer and the evader have different kinematic constraints than a Dubins car, the players' motion strategies in that work differ from those found in our current work. Additionally, dealing with two non-holonomic players requires using a higher dimensional space representation, which makes the analysis harder to perform.

A differential game of surveillance between two identical Dubins cars was studied in [30]. That work presents a partial solution to the problem where the pursuer is equipped with a circular detection region. Like our work, the pursuer wants to keep the evader inside its detection region as much as possible, while the evader has the opposite goal. However, different from [30], the pursuer has a semi-infinite conic detection region in our game. It is important to stress that this change

directly impacts the evader's escape condition. In [30], the escape is attained when the evader reaches a certain distance from the pursuer, while, in our current work, it is accomplished when the relative orientation of the evader from the pursuer's location is greater than the angle defining the semi-infinite cone. That may seem like a minor difference; however, it has been systematically observed in differential games' literature that altering the sensor's constraints requires a new problem analysis since the players' motion strategies to achieve their goals and the singular surfaces appearing in the game change.

In [31], another pursuit-evasion game of surveillance is analyzed. In that work, a Dubins car pursuer wants to maintain an Omnidirectional Agent inside its detection region. Like our work, the pursuer is equipped with a limited field of view sensor modeled as a semi-infinite cone. However, since the evader in that case is an Omnidirectional Agent, the players' motion strategies differ from the ones found in our current work. As was pointed out before, having two Dubins cars as players also implies requiring a higher dimensional space representation of the problem than the one in [31], which makes finding a solution a more difficult problem.

#### A. Contributions

The main contributions of this work are:

- We compute the players' time-optimal motion strategies near the game's end. The corresponding trajectories are described by analytical expressions.
- We reveal the existence of two singular surfaces: a Transition Surface, where one of the players switches its control, and an Evader's Universal Surface. We also found the players' motion strategies and the corresponding trajectories that reach those surfaces.
- We exhibit that the usual procedure of constructing the barrier from the boundary of the usable part to determine the game's winner is not enough in this case.

### III. PROBLEM DEFINITION

Two identical Dubins cars with unit speed and unit turn radius move on a plane without obstacles. One of them plays as the *pursuer*, and it is equipped with a limited field-of-view (FoV) detection region modeled as a semi-infinite cone with its apex at the pursuer's position. The pursuer aims to maintain the other Dubins car, which plays as the *evader*, as much time as possible inside its detection region. On the contrary, the evader wants to escape as soon as possible. The pursuer's FoV is modeled as a semi-infinite cone with half-angle  $\phi_d$  fixed to its location and aligned with its heading (see Fig. 1a). In this work, only kinematic constraints are considered.

We employ two representations to analyze and display the player's motion strategies. In the first one, which is known as *the realistic space* and we use Cartesian coordinates,  $(x_p, y_p, \theta_p)$  represents the pursuer's pose, and  $(x_e, y_e, \theta_e)$  represents the evader's pose (see Fig. 1a). Thus, the state of the system can be denoted as  $\mathbf{x} = (x_p, y_p, \theta_p, x_e, y_e, \theta_e) \in \mathbb{R}^2 \times S^1 \times$

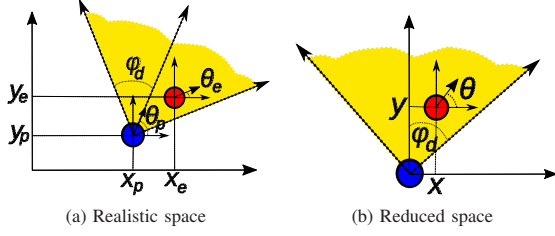


Fig. 1. The pursuer and the evader are represented by the blue and red dots, respectively.

$\mathbb{R}^2 \times S^1$ . The following equations describe the players' motions in the realistic space

$$\begin{aligned} \dot{x}_p &= \cos \theta_p, \quad \dot{y}_p = \sin \theta_p, \quad \dot{\theta}_p = v_p, \\ \dot{x}_e &= \cos \theta_e, \quad \dot{y}_e = \sin \theta_e, \quad \dot{\theta}_e = v_e, \end{aligned} \quad (1)$$

where  $v_p \in [-1, 1]$  is the pursuer's control and  $v_e \in [-1, 1]$  corresponds to the evader's control. All angles are measured counter-clockwise from the positive  $x$ -axis in this representation (see Fig. 1a).

In the second representation, we employ a coordinate transformation in which the reference frame is fixed to the pursuer's location, and the  $y$ -axis is aligned with its motion direction (see Fig. 1b). All angles are measured in a clockwise direction from the  $y$ -axis. This representation is known as *the reduced space*, and it is obtained using the following coordinate transformation

$$\begin{aligned} x &= (x_e - x_p) \sin \theta_p - (y_e - y_p) \cos \theta_p, \\ y &= (x_e - x_p) \cos \theta_p + (y_e - y_p) \sin \theta_p, \\ \theta &= \theta_p - \theta_e. \end{aligned} \quad (2)$$

The system's state in the reduced space is denoted as  $\mathbf{x}_R = (x, y, \theta)$ . Computing the time derivative of (2), we get the following kinematic equations

$$\dot{x} = v_p y + \sin \theta, \quad \dot{y} = -v_p x - 1 + \cos \theta, \quad \dot{\theta} = v_p - v_e, \quad (3)$$

where again  $v_e, v_p \in [-1, 1]$  denote the pursuer's and the evader's controls, respectively. They can be expressed as  $\dot{\mathbf{x}}_R = f(\mathbf{x}_R, v_e, v_p)$ . Having a cylindrical representation of the state  $\mathbf{x}_c = (r, \phi, \theta)$  in the reduced space is also convenient. Here,  $r$  is the distance from the origin to the evader's location,  $\phi$  is the angle between the pursuer's heading ( $y$ -axis) and the evader's location, and  $\theta$  is defined in the same way as in (2). The kinematic equations of the cylindrical representation are given by

$$\begin{aligned} \dot{r} &= \cos(\theta - \phi) - \cos \phi, \quad \dot{\phi} = v_p + \frac{\sin(\theta - \phi) + \sin \phi}{r}, \\ \dot{\theta} &= v_p - v_e. \end{aligned} \quad (4)$$

In this work, during the analysis of the problem, we indistinctly switch between the two coordinate representations of the state in the reduced space.

In Fig. 1b, we can observe that the conic detection region is split into two symmetric parts by the  $y$ -axis. In the following paragraphs, we describe the construction of motion strategies

in the right part of the semi-infinite cone, i.e.,  $\phi \in [0, \phi_d]$ . The trajectories in the left part, i.e.,  $\phi \in [-\phi_d, 0]$  can be obtained employing some symmetries around the  $y$ -axis.

#### IV. TERMINAL CONDITIONS

One fundamental step in solving a differential game is to find the initial conditions used to perform the retro-time integration of the motion equations [1], [2], [3]. In our game, those configurations where the evader is located at the right boundary of the conic detection region  $\phi = \phi_d$  and can increase the value of  $\phi$  regardless of the controls applied by the pursuer are used as initial conditions and are called the *usable part* (UP). The following equation represents the previous condition

$$\text{UP} = \left\{ (r, \phi_d, \theta) : \min_{v_p} \max_{v_e} \dot{\phi} > 0 \right\}, \quad (5)$$

or

$$\text{UP} = \left\{ (r, \phi_d, \theta) : \min_{v_e} \max_{v_p} -\dot{\phi} < 0 \right\}, \quad (6)$$

to follow the convention in the problem definition that the pursuer is the maximizer player, and the evader is the minimizer player. Substituting (4) into (6), we get

$$\text{UP} = \left\{ (r, \phi_d, \theta) : \min_{v_e} \max_{v_p} \left[ -v_p - \frac{\sin(\theta - \phi_d) - \sin \phi_d}{r} < 0 \right] \right\}. \quad (7)$$

For  $\phi_d \in [0, \frac{\pi}{2}]$ , we found that  $v_p = -1$  maximizes (7). Also, note that  $\dot{\phi}$  is independent of the value of  $v_e$ . Substituting  $v_p = -1$  into (7) we get

$$\text{UP} = \left\{ (r, \phi_d, \theta) : 1 - \frac{\sin(\theta - \phi_d) - \sin \phi_d}{r} < 0 \right\}. \quad (8)$$

By doing some algebraic manipulation, we found that

$$\text{UP} = \left\{ (r, \phi_d, \theta) : r < \sin(\theta - \phi_d) + \sin \phi_d \right\}. \quad (9)$$

The *boundary of the usable part* (BUP) corresponds to those configurations

$$\text{BUP} = \left\{ (r, \phi_d, \theta) : r = \sin(\theta - \phi_d) + \sin \phi_d \right\}, \quad (10)$$

where neither of the players can increase or decrease the value of  $\phi$ . From (10), we have that,  $r = 0$  at  $\theta = 0$  and  $\theta = \pi + 2\phi_d$ , and  $r = 1 + \sin \phi_d$  (maximum value) at  $\theta = \pi/2 + \phi_d$ . Fig. 2 shows a representation of the UP and the BUP, for  $\phi_d = 40^\circ$ .

#### V. MOTION STRATEGIES

In this section, we compute the players' optimal strategies to attain their goals in the right portion of the semi-infinite cone, i.e.,  $\phi \in [0, \phi_d]$ . Following the methodology described in [1], [2], [3], a retro-time integration of the players' motion equations is performed, taking the configurations at the UP as initial conditions. In the following, we denote the retro-time as  $\tau = t_f - t$ , where  $t_f$  is the termination time of the game.

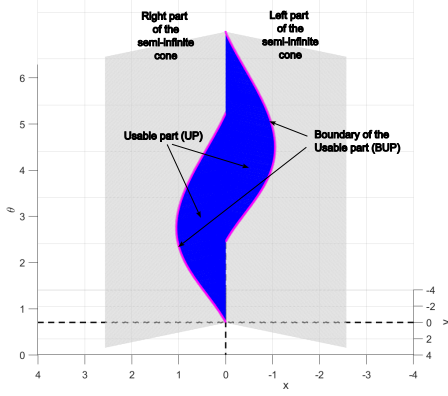


Fig. 2. Representation of the Usable Part (UP), blue region, and its boundary (BUP), magenta curves, in the reduced space for  $\phi_d = 40^\circ$ . The gray rectangles represent the semi-infinite cone as  $\theta$  varies from 0 to  $2\pi$ . The image shows a view from an observer located in front of the semi-infinite cone.

### A. Optimal controls

First, we need to find the expressions of the optimal controls used by the players during the game. To do that, we have to construct the Hamiltonian of the system. From [2], we have that

$$H(\mathbf{x}, \lambda, v_e, v_p) = \lambda^T \cdot f(\mathbf{x}, v_e, v_p) + L(\mathbf{x}, v_e, v_p), \quad (11)$$

where  $\lambda^T$  are the costate variables and  $L(\mathbf{x}, v_e, v_p)$  is the cost function. Recalling that  $L(\mathbf{x}, v_e, v_p) = 1$  for problems of minimum time [1], like the one addressed in this paper, and substituting (3) into (11), we have that in the reduced space and Cartesian coordinates

$$H(\mathbf{x}, \lambda, v_p, v_e) = \lambda_x v_p y + \lambda_x \sin \theta - \lambda_y v_p x - \lambda_y + \lambda_y \cos \theta + \lambda_\theta v_p - \lambda_\theta v_e + 1. \quad (12)$$

The optimal controls are obtained from (12) and Pontryagin's Maximum Principle, which states that along the systems' optimal trajectories

$$\begin{aligned} \min_{v_e} \max_{v_p} H(\mathbf{x}, \lambda, v_e, v_p) &= 0, \\ v_e^* &= \arg \min_{v_e} H(\mathbf{x}, \lambda, v_e, v_p), \quad v_p^* = \arg \max_{v_p} H(\mathbf{x}, \lambda, v_e, v_p), \end{aligned} \quad (13)$$

where  $v_p^*$  and  $v_e^*$  denote the optimal controls of the pursuer and the evader, respectively. Thus, we have that the pursuer's optimal control in the reduced space and Cartesian coordinates is given by

$$v_p^* = \text{sgn}(y\lambda_x - x\lambda_y + \lambda_\theta), \quad (14)$$

and the evader's optimal control by

$$v_e^* = \text{sgn}(\lambda_\theta). \quad (15)$$

### B. Costate equation

From (14) and (15), one can notice that for computing the players' optimal controls, we require to know the values of  $\lambda^T = [\lambda_x \ \lambda_y \ \lambda_\theta]^T$  as time elapses. To find those values, we

use the costate equation. In particular, since we are going to perform a retro-time integration of the motion equations, we have to use the retro-time version of the costate equation

$$\dot{\lambda} = \frac{\partial}{\partial x} H(\mathbf{x}, \lambda, v_e^*, v_p^*), \quad (16)$$

where the retro-time derivative of a variable  $x$  is represented by  $\dot{x}$ . Substituting (3) into (16), and considering the players' optimal controls  $v_e^*$  and  $v_p^*$  we have that

$$\dot{\lambda}_x = -v_p^* \lambda_y, \quad \dot{\lambda}_y = v_p^* \lambda_x, \quad \dot{\lambda}_\theta = \lambda_x \cos \theta - \lambda_y \sin \theta. \quad (17)$$

We need to find the initial conditions at the game's end ( $\tau = 0$ ) to perform the retro-time integration of (17). Recalling that at the UP,  $x = r \sin \phi_d$ ,  $y = r \cos \phi_d$  and  $\theta = \theta_d$ , from the traversability conditions we have that

$$\lambda_x = -\cos \phi_d, \quad \lambda_y = \sin \phi_d, \quad \lambda_\theta = 0. \quad (18)$$

Integrating (17) considering the initial conditions in (18), we have that

$$\begin{aligned} \lambda_x &= -\cos(\phi_d - v_p^* \tau), \quad \lambda_y = \sin(\phi_d - v_p^* \tau), \\ \lambda_\theta &= v_e^* (-\sin(\phi_d - \theta_d) + \sin(\phi_d - \theta_d - v_e^* \tau)). \end{aligned} \quad (19)$$

### C. Primary solution

Now, we compute the trajectories of the players that lead directly to the terminal conditions (see Fig. 3). Those trajectories are known as the *primary solution*. To compute those trajectories, we need the retro-time version of the motion equations

$$\dot{x} = -v_p y - \sin \theta, \quad \dot{y} = v_p x + 1 - \cos \theta, \quad \dot{\theta} = -v_p + v_e. \quad (20)$$

Integrating (20), considering the initial conditions  $x = r \sin \phi_d$ ,  $y = r \cos \phi_d$  and  $\theta = \theta_d$  at the UP, and the players' optimal controls  $v_p^*$  and  $v_e^*$ , we have that

$$\begin{aligned} x &= -v_p^* + v_p^* \cos(v_p^* \tau) - v_e^* \cos(\theta_d - v_p^* \tau) \\ &\quad + v_e^* \cos(\theta_d + (v_e^* - v_p^*) \tau) + r \sin(\phi_d - v_p^* \tau), \\ y &= v_p^* \sin(v_p^* \tau) + r \cos(\phi_d - v_p^* \tau) \\ &\quad - 2v_e^* \cos\left(\theta_d + \left(\frac{v_e^*}{2} - v_p^*\right) \tau\right) \sin\left(\frac{v_e^*}{2} \tau\right), \\ \theta &= \theta_d + (v_e^* - v_p^*) \tau. \end{aligned} \quad (21)$$

This solution is valid as long as the players do not switch controls. In this game, we found that after the players follow the previous trajectories for some time, the pursuer switches its control. We discuss this behavior later in the paper.

### D. Discussion of the previous solution

Note that  $\lambda_\theta = 0$  at the game's end, then from (15),  $v_e^* = 0$ . Thus, we must check whether the evader continues using that control or switches it immediately. We can do that by analyzing the value of  $\dot{\lambda}_\theta$  at the game's end.

Substituting the terminal conditions  $x = r \sin \phi_d$ ,  $y = r \cos \phi_d$  and  $\theta = \theta_d$  into (17), we have that

$$\dot{\lambda}_\theta = -\cos(\phi_d - \theta_d). \quad (22)$$



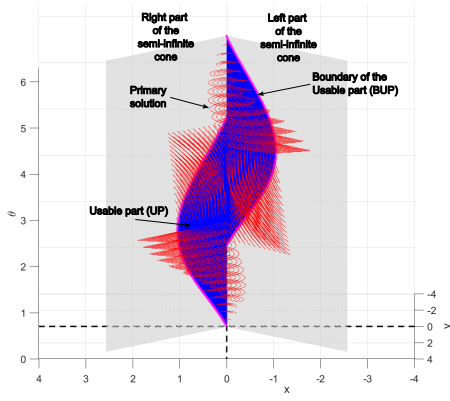


Fig. 3. An example of the primary solution (red curves) for  $\phi_d = 40^\circ$ .

From (22), we can deduce that  $\dot{\lambda}_\theta \neq 0$  for any value of  $\phi_d - \theta_d \neq \frac{\pi}{2}$ . This implies that in those cases, we can use the sign of  $\dot{\lambda}_\theta$  to compute the control of  $v_e^*$  immediately before the game's end and substitute its value in (20) and (21).

For  $\phi_d - \theta_d = \frac{\pi}{2}$ , we can check whether  $\dot{\lambda}_\theta$  is different from zero. From (17), and recalling again that  $r = \sin \phi_d$ ,  $r = \cos \phi_d$  and  $\theta = \theta_d$  at the game's end, we found that

$$\ddot{\lambda}_\theta = v_e^*. \quad (23)$$

Note that the previous expression depends on  $v_e^*$ . From the definition of the sgn function,  $v_e^*$  can take the values  $-1$ ,  $0$ , and  $-1$ . As described in previous works [1], [4], [30], this suggests the existence of an Evader's Universal Surface (EUS). On that surface, the evader applies  $v_e^* = 0$ , which can be verified using Isaacs' necessary condition for the existence of Universal Surfaces [1].

#### E. Evader's Universal Surface and its tributary trajectories

In this section, we construct the trajectories corresponding to the EUS (see Fig. 4). Recalling that  $v_e^* = 0$ , we have the retro-time version of the motion equations take the form

$$\dot{x} = -v_p y - \sin \theta, \quad \dot{y} = v_p x + 1 - \cos \theta, \quad \dot{\theta} = -v_p. \quad (24)$$

Integrating (24), considering the initial conditions  $x = r \sin \phi_d$ ,  $y = r \cos \phi_d$  and  $\theta_d = \phi_d - \frac{\pi}{2}$  at the UP, and the players' optimal controls, we get

$$\begin{aligned} x &= -v_p^* + v_p^* \cos(v_p^* \tau) + r \sin(\phi_d - v_p^* \tau) - \tau \sin(\theta_d - v_p^* \tau), \\ y &= v_p^* \sin(v_p^* \tau) + r \cos(\phi_d - v_p^* \tau) - \tau \cos(\theta_d - v_p^* \tau), \\ \theta &= \theta_d - v_p^* \tau. \end{aligned} \quad (25)$$

From the traversability conditions, in this case, we have that

$$\lambda_x = -\cos \phi_d, \quad \lambda_y = \sin \phi_d, \quad \lambda_\theta = 0. \quad (26)$$

Integrating (17) considering the initial conditions in (26), we get

$$\lambda_x = -\cos(\phi_d - v_p^* \tau), \quad \lambda_y = \sin(\phi_d - v_p^* \tau), \quad \lambda_\theta = 0. \quad (27)$$

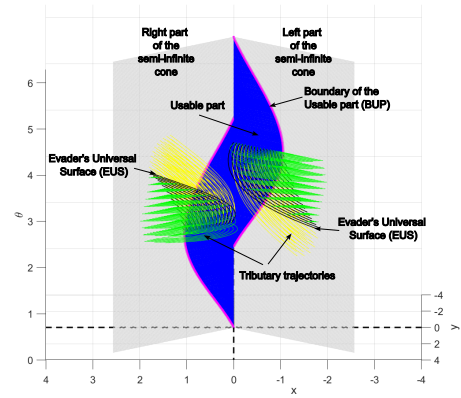


Fig. 4. An example of the Evader's Universal Surface (black curves) and its tributary trajectories for  $\phi_d = 40^\circ$ . The green and yellow colors indicate the trajectories at each side of the EUS. The evader applies a particular control at each side, i.e.,  $v_e^* = -1$  or  $v_e^* = 1$ .

1) *Tributary trajectories*: Now, we compute the tributary trajectories reaching the EUS (see Fig. 4). In this case, the retro-time version of the motion equations is

$$\dot{x} = -v_p y - \sin \theta, \quad \dot{y} = v_p x + 1 - \cos \theta, \quad \dot{\theta} = -v_p + v_e. \quad (28)$$

Integrating (28), considering as initial conditions the configurations  $(x_{US}, y_{US}, \theta_{US})$  at the EUS, and the players' optimal controls, we have that

$$\begin{aligned} x &= -v_p^* + v_p^* \cos(v_p^*(\tau - \tau_{US})) - v_e^* \cos(\theta_{US} - v_p^*(\tau - \tau_{US})) \\ &\quad + v_e^* \cos(\theta_{US} + (v_e^* - v_p^*)(\tau - \tau_{US})) + r_{US} \sin(\phi_{US} - v_p^*(\tau - \tau_{US})), \\ y &= v_p^* \sin(v_p^*(\tau - \tau_{US})) + r_{US} \cos(\phi_{US} - v_p^*(\tau - \tau_{US})) \\ &\quad - 2v_e^* \cos\left(\theta_{US} + \left(\frac{v_e^*}{2} - v_p^*\right)(\tau - \tau_{US})\right) \sin\left(\frac{v_e^*}{2}(\tau - \tau_{US})\right), \\ \theta &= \theta_{US} + (v_e^* - v_p^*)(\tau - \tau_{US}), \end{aligned} \quad (29)$$

where  $(r_{US}, \phi_{US}, \theta_{US})$  are the cylindrical coordinates of  $(x_{US}, y_{US}, \theta_{US})$  and  $\tau_{US}$  is retro-time elapsed to reach those configurations. In this case, we have that

$$\begin{aligned} \lambda_x &= -\cos(\phi_d - v_p^* \tau), \quad \lambda_y = \sin(\phi_d - v_p^* \tau), \\ \lambda_\theta &= v_e^* (-\sin(\phi_d - \theta_d) + \sin(\phi_d - \theta_d - v_e^*(\tau - \tau_{US}))), \end{aligned} \quad (30)$$

for  $\tau \geq \tau_{US}$ . Note that the evader applies a particular control at each side of the EUS, i.e.,  $v_e^* = -1$  or  $v_e^* = 1$ .

The previous equations are valid as long as the players do not switch controls. Similarly to the primary surface, we found that the pursuer switches its control after some time.

#### F. Transition Surface at the primary solution

As mentioned before, we found that the pursuer switches control after some time when the system follows the primary solution (see Fig. 5). We denote this time as  $\tau_s$  and the configurations in the playing space where this change occurs belong to the Transition Surface (TS). Since transcendental equations describe the motion trajectories in the primary solution, we did not find an analytical expression for  $\tau_s$ . Thus,

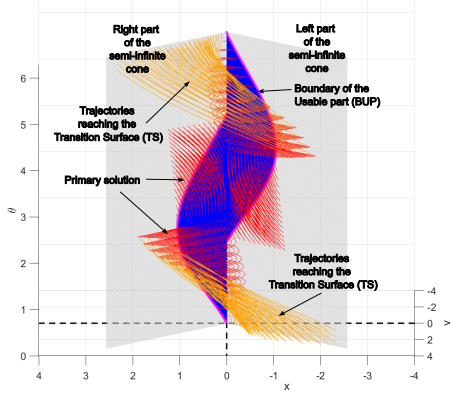


Fig. 5. An example of the trajectories reaching the Transition Surface (orange curves) for  $\phi_d = 40^\circ$ . The Transition surface corresponds to the points where the orange curves meet the primary solution (red curves).

we employ numerical analysis to determine its value. When the system reaches  $\tau_s$ , we need to perform a new integration of the costate and motion equations taking as initial conditions the values of  $\lambda_x$ ,  $\lambda_y$ ,  $\lambda_\theta$ ,  $x$ ,  $y$  and  $\theta$  at  $\tau_s$ . In this case, the costate variables are given by the following expressions

$$\begin{aligned}\lambda_x &= -\cos(\phi_d - v_{p0}^* \tau_s - v_p^*(\tau - \tau_s)), \\ \lambda_y &= \sin(\phi_d - v_{p0}^* \tau_s - v_p^*(\tau - \tau_s)), \\ \lambda_\theta &= v_e^*(-\sin(\phi_d - \theta_d) + \sin(\phi_d - \theta_d - v_e^* \tau)),\end{aligned}\quad (31)$$

where  $v_{p0}^*$  denotes the pursuer's optimal control before the switch and  $v_p^*$  is the pursuer's optimal control after the switch. For  $\phi \in [0, \frac{\pi}{2}]$ , we that  $v_p^*$  switches from  $-1$  to  $1$ , i.e.,  $v_{p0} = -1$  and  $v_p^* = 1$  after the switch.

Integrating the motion equations, we get that

$$\begin{aligned}x &= -v_p^* + v_p^* \cos(v_p^*(\tau - \tau_s)) - v_e^* \cos(\theta_s - v_p^*(\tau - \tau_s)) \\ &\quad + v_e^* \cos(\theta_s + (v_e^* - v_p^*)(\tau - \tau_s)) + r_s \sin(\phi_s - v_p^*(\tau - \tau_s)), \\ y &= v_p^* \sin(v_p^*(\tau - \tau_s)) + r_s \cos(\phi_s - v_p^*(\tau - \tau_s)) \\ &\quad - 2v_e^* \cos\left(\theta_s + \left(\frac{v_e^*}{2} - v_p^*\right)(\tau - \tau_s)\right) \sin\left(\frac{v_e^*}{2}(\tau - \tau_s)\right), \\ \theta &= \theta_s + (v_e^* - v_p^*)(\tau - \tau_s),\end{aligned}\quad (32)$$

where  $(r_s, \phi_s, \theta_s)$  are the cylindrical coordinates of the system's state at time  $\tau_s$  in the primary solution. Those expressions provide the trajectories emanating from the TS in retro-time.

#### G. Transition Surface at the tributary trajectories of the Evader's Universal Surface

Similarly to the previous case, we found that for some tributary trajectories of the EUS, the pursuer switches control after some time  $\tau_{s'}$  (see Fig. 6). Thus, we need to perform a new integration of the motion and adjoint equations. Again, since the tributary trajectories are described by transcendental equations, we cannot find an analytical expression for  $\tau_{s'}$ .

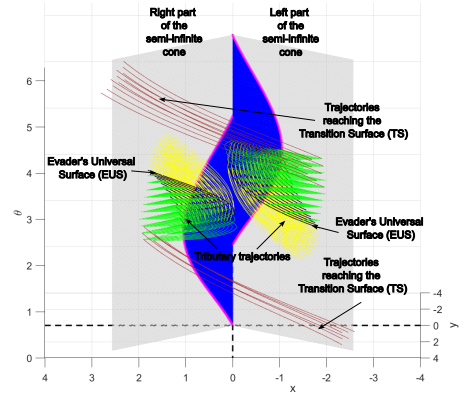


Fig. 6. An example of the trajectories reaching the Transition Surface (brown curves) at the Evader's Universal Surface tributary trajectories for  $\phi_d = 40^\circ$ . The Transition Surface corresponds to the points where the brown curves meet the tributary trajectories (yellow and green curves).

However, it can be computed numerically. Performing a new integration of the motion equations we have that

$$\begin{aligned}x &= -v_p^* + v_p^* \cos(v_p^*(\tau - \tau_{s'})) - v_e^* \cos(\theta_{s'} - v_p^*(\tau - \tau_{s'})) \\ &\quad + v_e^* \cos(\theta_{s'} + (v_e^* - v_p^*)(\tau - \tau_{s'})) + r_{s'} \sin(\phi_{s'} - v_p^*(\tau - \tau_{s'})), \\ y &= v_p^* \sin(v_p^*(\tau - \tau_{s'})) + r_{s'} \cos(\phi_{s'} - v_p^*(\tau - \tau_{s'})) \\ &\quad - 2v_e^* \cos\left(\theta_{s'} + \left(\frac{v_e^*}{2} - v_p^*\right)(\tau - \tau_{s'})\right) \sin\left(\frac{v_e^*}{2}(\tau - \tau_{s'})\right), \\ \theta &= \theta_{s'} + (v_e^* - v_p^*)(\tau - \tau_{s'}),\end{aligned}\quad (33)$$

where  $(r_{s'}, \phi_{s'}, \theta_{s'})$  are the cylindrical coordinates of the system's state at time  $\tau_{s'}$  in the tributary trajectory. The costate variables are given by

$$\begin{aligned}\lambda_x &= -\cos(\phi_d - v_{p0}^* \tau_{s'}' - v_p^*(\tau - \tau_{s'}')), \\ \lambda_y &= \sin(\phi_d - v_{p0}^* \tau_{s'}' - v_p^*(\tau - \tau_{s'}')), \\ \lambda_\theta &= v_e^*(-\sin(\phi_d - \theta_d) + \sin(\phi_d - \theta_d - v_e^*(\tau - \tau_{US}))),\end{aligned}\quad (34)$$

where  $v_{p0}^*$  denotes the pursuer's optimal control before the switch and  $v_p^*$  is the pursuer's optimal control after the switch. For  $\phi \in [0, \frac{\pi}{2}]$ , we that  $v_p^*$  switches from  $-1$  to  $1$ , i.e.,  $v_{p0} = -1$  and  $v_p^* = 1$  after the switch.

## VI. AN ATTEMPT TO SOLVE THE DECISION PROBLEM

One of the main questions addressed when solving a pursuit-evasion game is determining the game's winner. In our problem, that means finding the region of initial configurations where the evader can escape surveillance and those where is impossible. In differential game theory, the curve separating those regions is known as *the barrier* [1]. A similar approach to the one followed in the previous section is used to find the barrier. In this case, a retro-time integration of the costate and motion equations is performed, taking the configurations at the BUP as initial conditions.

We found that the barrier's standard construction produces a surface that partially lies outside the playing space and

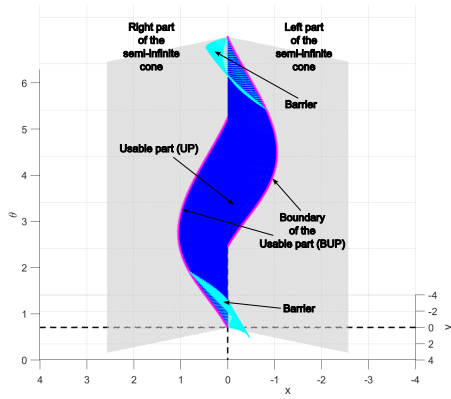


Fig. 7. Representation of the barrier (cyan curves) for  $\phi_d = 40^\circ$ . We can observe that some configurations at the BUP do not have a trajectory reaching it. The reason behind this is that the retro-integration of the motion equations starting from those configurations produces trajectories outside the semi-infinite cone, and thus, they are invalid.

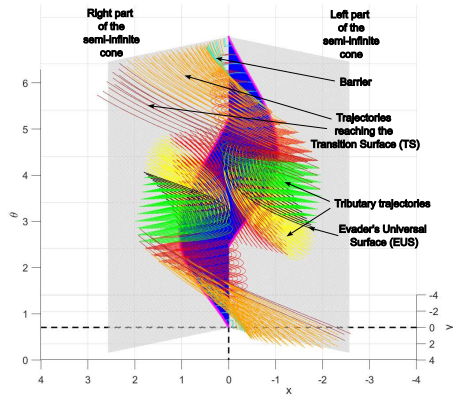


Fig. 8. An overview of the trajectories found in this work near the game's end for  $\phi_d = 40^\circ$ .

needs to be discarded. Fig. 7 shows a representation of the barrier. In that figure, we can observe that only a subset of the configurations belonging to the BUP has a barrier trajectory that goes into the playing space and those trajectories fail to define a closed region. This suggests that the evader can escape from all initial positions in the playing space or that the playing space is bounded by other barrier surfaces that also emerge from constructing additional singular surfaces. Unfortunately, in this paper, we have not discovered which of the previous two cases occurs since the task has proved to be very complex. In particular, the process of discovering additional singular surfaces is challenging since the trajectories found so far are represented by the transcendental equations.

## VII. DISCUSSION OF THE MOTION STRATEGIES NEAR THE GAME'S END

Fig. 8 presents the set of motion strategies and their corresponding trajectories near the game's end. We can observe that the current trajectories are not enough to cover the entire playing space. Similar to the barrier case, this behavior suggests

that additional singular surfaces must be found in the current problem. However, as pointed out before, finding them is an intricate task that may require a lot of algebraic manipulations and presumably numerical analysis. Recall that all players' trajectories presented in this work were obtained analytically, and they are represented by transcendental equations. From Fig. 8, we can notice that the tributary trajectories of the Evader's Universal Surface join smoothly with the trajectories of the primary solution. The same behavior can be observed with the trajectories reaching the Transition Surface. That indicates that the solutions seam those regions.

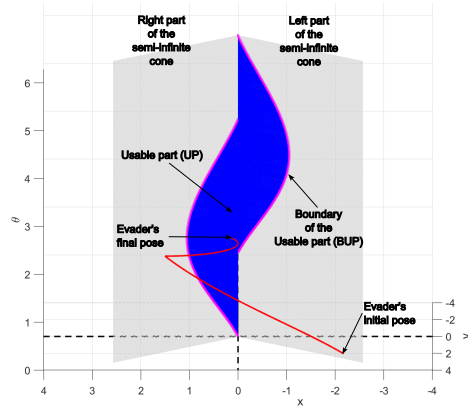
## VIII. SIMULATION

This section presents a numerical simulation to illustrate the players' motion strategies. The parameters for the simulation are  $\phi_d = 40^\circ$  and  $\theta_d = 120^\circ$ . In the example, the evader starts at the left boundary of the detection region (see Fig. 9a). In the reduced space, the system follows a trajectory that reaches the Transition Surface and continues to the terminal condition, traveling a trajectory of the primary solution. In the realistic space (see Fig. 9b), the evader seeks to get closer to the pursuer and reach the right boundary of the detection region. Note that since the evader's initial orientation is pointing toward the interior of the detection region, and it cannot move backward, it cannot escape immediately despite being located at the left boundary. The pursuer takes advantage of this, first moving in a way that puts the evader in the center of the detection region, and later pushing the right boundary away from the evader. However, despite the pursuer's efforts, the evader can reach the right boundary of the detection region.

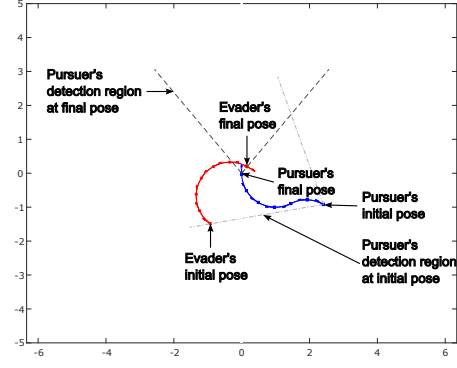
## IX. CONCLUSIONS AND FUTURE WORK

In this work, we studied the differential game of keeping surveillance of a Dubins car with an identical Dubins car equipped with a limited field of view sensor, modeled as a semi-infinite cone fixed to its body. The evader wants to escape from the detection region as soon as possible. On the contrary, the pursuer wants to keep surveillance of the evader as much as possible. We found the players' time-optimal motion strategies near the game's end. The analysis of the trajectories reveals the existence of at least two singular surfaces: a Transition Surface and an Evader's Universal Surface. We also found the players' motion strategies and the corresponding trajectories that reach those surfaces. We presented a numerical example of the players' motion strategies.

Additionally, we encountered that the barrier's standard construction fails to solve the problem of deciding the game's winner. In particular, we found that it produces a surface that partially lies outside the playing space. This suggests that 1) either the evader can escape from all initial positions in the playing space, in which case additional singular surfaces and their corresponding trajectories need to be found to fill the entire playing space, or 2) the playing space is bounded by other barrier surfaces that emerge from constructing additional singular surfaces. Unfortunately, in this work, we cannot determine analytically which of the previous two cases occurs



(a) Trajectory of the system in the reduced space.



(b) Trajectory of the system in the realistic space. The blue curve indicates the pursuer's trajectory and the red curve indicates the evader's trajectory. Arrows show the players' motion directions.

Fig. 9. Results of the numerical simulation.

since the task has proved to be very complex. However, this paper presents the first study of the proposed pursuit-evasion problem and establishes the foundations for future analysis.

## REFERENCES

- [1] R. Isaacs, *Differential games: a mathematical theory with applications to warfare and pursuit, control and optimization*. Courier Corporation, 1999.
- [2] T. Başar and G. J. Olsder, *Dynamic noncooperative game theory*. SIAM, 1998.
- [3] J. Lewin, *Differential games: theory and methods for solving game problems with singular surfaces*. Springer Science & Business Media, 2012.
- [4] A. Merz, "The game of two identical cars," *Journal of Optimization Theory and Applications*, vol. 9, pp. 324–343, 1972.
- [5] A. W. Merz, "The homicidal chauffeur," *AIAA Journal*, vol. 12, no. 3, pp. 259–260, 1974.
- [6] L. J. Guibas, J.-C. Latombe, S. M. LaValle, D. Lin, and R. Motwani, "A visibility-based pursuit-evasion problem," *International Journal of Computational Geometry & Applications*, vol. 9, no. 04n05, pp. 471–493, 1999.
- [7] B. Tovar and S. M. LaValle, "Visibility-based pursuit—evasion with bounded speed," *The International Journal of Robotics Research*, vol. 27, no. 11-12, pp. 1350–1360, 2008.
- [8] G. Hollinger, S. Singh, J. Djughash, and A. Kehagias, "Efficient multi-robot search for a moving target," *The International Journal of Robotics Research*, vol. 28, no. 2, pp. 201–219, 2009.
- [9] N. Karnad and V. Isler, "Lion and man game in the presence of a circular obstacle," in *2009 IEEE/RSJ International Conference on Intelligent Robots and Systems*. IEEE, 2009, pp. 5045–5050.
- [10] U. Ruiz, R. Murrieta-Cid, and J. L. Marroquin, "Time-optimal motion strategies for capturing an omnidirectional evader using a differential drive robot," *IEEE Transactions on Robotics*, vol. 29, no. 5, pp. 1180–1196, 2013.
- [11] W. Li, "A dynamics perspective of pursuit-evasion: Capturing and escaping when the pursuer runs faster than the agile evader," *IEEE Transactions on Automatic Control*, vol. 62, no. 1, pp. 451–457, 2016.
- [12] R. Bera, V. R. Makkapati, and M. Kothari, "A comprehensive differential game theoretic solution to a game of two cars," *Journal of Optimization Theory and Applications*, vol. 174, pp. 818–836, 2017.
- [13] L. Bravo, U. Ruiz, and R. Murrieta-Cid, "A pursuit-evasion game between two identical differential drive robots," *Journal of the Franklin Institute*, vol. 357, no. 10, pp. 5773–5808, 2020.
- [14] R. Yan, X. Duan, Z. Shi, Y. Zhong, and F. Bullo, "Matching-based capture strategies for 3d heterogeneous multiplayer reach-avoid differential games," *Automatica*, vol. 140, p. 110207, 2022.
- [15] U. Ruiz, "Capturing a dubins car with a differential drive robot," *IEEE Access*, vol. 10, pp. 81 805–81 815, 2022.
- [16] A. Chaudhari and D. Chakraborty, "A time-optimal feedback control for a particular case of the game of two cars," *IEEE Transactions on Automatic Control*, vol. 67, no. 4, pp. 1806–1821, 2021.
- [17] B. P. Gerkey, S. Thrun, and G. Gordon, "Visibility-based pursuit-evasion with limited field of view," *The International Journal of Robotics Research*, vol. 25, no. 4, pp. 299–315, 2006.
- [18] S. Bhattacharya and S. Hutchinson, "On the existence of nash equilibrium for a two-player pursuit—evasion game with visibility constraints," *The International Journal of Robotics Research*, vol. 29, no. 7, pp. 831–839, 2010.
- [19] R. Murrieta-Cid, U. Ruiz, J. L. Marroquin, J.-P. Laumond, and S. Hutchinson, "Tracking an omnidirectional evader with a differential drive robot," *Autonomous Robots*, vol. 31, pp. 345–366, 2011.
- [20] I. Becerra, R. Murrieta-Cid, R. Monroy, S. Hutchinson, and J.-P. Laumond, "Maintaining strong mutual visibility of an evader moving over the reduced visibility graph," *Autonomous Robots*, vol. 40, pp. 395–423, 2016.
- [21] N. M. Stiffler and J. M. O'Kane, "Complete and optimal visibility-based pursuit-evasion," *The International Journal of Robotics Research*, vol. 36, no. 8, pp. 923–946, 2017.
- [22] R. Zou and S. Bhattacharya, "On optimal pursuit trajectories for visibility-based target-tracking game," *IEEE Transactions on Robotics*, vol. 35, no. 2, pp. 449–465, 2018.
- [23] U. Ruiz, "A game of surveillance between an omnidirectional agent and a differential drive robot," *International Journal of Control*, vol. 95, no. 6, pp. 1694–1706, 2022.
- [24] E. Lozano, I. Becerra, U. Ruiz, L. Bravo, and R. Murrieta-Cid, "A visibility-based pursuit-evasion game between two nonholonomic robots in environments with obstacles," *Autonomous Robots*, vol. 46, no. 2, pp. 349–371, 2022.
- [25] E. Lozano, U. Ruiz, I. Becerra, and R. Murrieta-Cid, "Surveillance and collision-free tracking of an aggressive evader with an actuated sensor pursuer," *IEEE Robotics and Automation Letters*, vol. 7, no. 3, pp. 6854–6861, 2022.
- [26] U. Ruiz, "Surveillance evasion between two identical differential drive robots," *European Journal of Control*, p. 100935, 2023.
- [27] T. H. Chung, G. A. Hollinger, and V. Isler, "Search and pursuit-evasion in mobile robotics: A survey," *Autonomous robots*, vol. 31, pp. 299–316, 2011.
- [28] C. Robin and S. Lacroix, "Multi-robot target detection and tracking: taxonomy and survey," *Autonomous Robots*, vol. 40, pp. 729–760, 2016.
- [29] U. Ruiz, "Time-optimal escape of an omnidirectional agent from the field of view of a differential drive robot," *International Journal of Control, Automation and Systems*, vol. 21, no. 1, pp. 292–305, 2023.
- [30] I. Greenfeld, "A differential game of surveillance evasion of two identical cars," *Journal of optimization theory and applications*, vol. 52, pp. 53–79, 1987.
- [31] J. Lewin and G. Olsder, "Conic surveillance evasion," *Journal of Optimization Theory and Applications*, vol. 27, pp. 107–125, 1979.